

Robust propagation direction of stresses in a minimal granular packing

D. A. Head,¹ A. V. Tkachenko² and T. A. Witten³

¹ Department of Physics and Astronomy, JCMB King's Buildings, University of Edinburgh, Edinburgh EH9 3JZ, UK

² Bell Labs, Lucent Technologies, 600-700 Mountain Ave., Murray Hill, NJ 07974, USA

³ The James Franck Institute, The University of Chicago, Chicago, Illinois 60637, USA

October 24, 2018

Abstract. By employing the adaptive network simulation method, we demonstrate that the ensemble-averaged stress caused by a local force for packings of frictionless rigid beads is concentrated along rays whose slope is consistent with unity: forces propagate along lines at 45 degrees to the horizontal or vertical. This slope is shown to be independent of polydispersity or the degree to which the system is sheared. Further confirmation of this result comes from fitting the components of the stress tensor to the null stress 'constitutive equation.' The magnitude of the response is also shown to fall off with the $-1/2$ power of distance. We argue that our findings are a natural consequence of a system that preserves its volume under small perturbations.

PACS. 45.70.Cc Static sandpiles; granular compaction – 83.80.Fg Granular solids; granular compaction

1 Introduction

It is becoming increasingly evident that the transmission of stress through a disordered body of incompressible, cohesionless beads obeys principles that are distinct from those of either elastic or elastoplastic materials [1,2,3,4,5,6]. Even defining a strain field for a granular body is problematic [1,2], let alone relating the strain to the stress

in a constitutive equation, as in elastic systems. Furthermore, experiments measuring the stress under conical and wedge-shaped sandpiles have indicated a pressure minimum below the apex when the material is poured from a point (or line) source, but not when it is sprinkled uniformly over the base [3]. This dependence on construction history is also quite unlike elastic or elastoplastic materials.

To circumvent the difficulties arising from an ill-defined strain, a class of ‘constitutive equations’ have been proposed that relate the independent components of the stress tensor σ_{ij} without reference to a displacement field [1,8,9]. (Note that, like many authors, we use the phrase ‘constitutive equation’ even in the absence of a well-defined strain field or history independence). In their most general form, these equations suppose that the σ_{ij} can be related in a linear expression, with coefficients that in general depend on the construction history of the pile. The basic form of these equations has also been confirmed by mean field analysis of frictionless spheres, where it was referred to as the ‘null stress’ law [10].

A remarkable feature of the proposed equations is that they are hyperbolic in form, and thus belong to the same class of equations as the wave equation. Hence they predict that the response to a localised perturbation should propagate outwards from the source of the disturbance in waves, with the direction of increasing depth playing the role of time. To test this prediction, experiments have recently been performed on systems of photoelastic discs that have a small load applied to the upper surface, and the stress response in the bulk measured [6]. These seemed to show wave-like propagation over all distances for low polydispersity, but only for short distances for high polydispersity. To further complicate the issue, similar experiments on sand have failed to show any trace of wave-like propagation whatsoever [7].

Until more experiments have been performed and a consensus reached, it is natural to turn to computer sim-

ulations for additional data. However, conventional simulation methods cannot directly probe the linear response regime and must instead apply a finite force, which runs the risk of perturbing the system. To this end, two of us (AT, TW) have devised a novel simulation method, called the ‘adaptive network algorithm,’ which directly probes the linear regime in a system of frictionless and rigid discs [11].

In this paper, we employ the adaptive network algorithm to investigate the stress response function in frictionless disc systems, and to ascertain if it obeys wave-like propagation. We begin by briefly describing the simulation method in Sec. 2, before demonstrating in Sec. 3 that the null-stress law is obeyed, with the stress tensor approximately obeying the relation $\sigma_{yy} = c^2\sigma_{xx}$ with $c \approx 1$. This result has already been found [11] for weakly polydisperse systems, with the same value of c ; here we extend the result to strong polydispersity.

The response function itself is analysed in Sec. 4, where it is shown to be concentrated along two ‘light rays’ that propagate outwards from the source of the disturbance. Furthermore, the same ‘speed of light’ $c \approx 1$ is found in all cases, irrespective of the direction of the perturbing force, the polydispersity of the system, or the degree to which the system is being sheared. This behaviour persists to the largest depths we have been able to simulate, typically around 10–15 bead diameters in the vertical direction, which is comparable with the experiments on photoelastic discs; however, they found no evidence of $c \approx 1$. In Sec. 5 we attempt to explain this discrepancy by arguing that

$c = 1$ corresponds to a system that conserves its volume under small perturbations. Finally, in Sec. 6 we summarise our results and suggest directions for future work.

2 Overview of the simulation method

The full derivation of the adaptive network algorithm and its associated assumptions has already been presented at length elsewhere [11]; here we only mention those details pertinent to the current work. The algorithm consists of two stages: firstly, a packing of discs is constructed, and secondly, the contact force network is generated in response to an applied load. We consider two-dimensional systems of frictionless discs α , with radii R_α that are uniformly distributed over the interval $[1, R_{\max}]$. The parameter $R_{\max} > 1$ will be used as a measure of the polydispersity of the system. The pile is built upon a fixed rough base, consisting of a row of discs belonging to the same size distribution as those deposited, and whose centres all have the same vertical coordinate. Periodic boundary conditions are obeyed in the horizontal direction. For computational efficiency, the beads are assumed to be weightless except for those at the free surface, which are subjected to a uniform load \mathbf{F}^{ext} . Here, \mathbf{F}^{ext} can point in a direction other than vertically downwards, thus allowing the system to be *sheared*.

The pack of discs is built by adding each successive disc at the lowest available point. Once added, each disc's centre remains fixed throughout the subsequent relaxation process. The sequential nature of the initial packing means that it is straightforward to calculate the contact forces

as the applied load propagates from the upper surface to the base; see [11] for details on how this is done. In general, some of the contact forces will be tensile and thus incompatible with a cohesionless medium. Therefore we now modify the contact network until all tensile bonds have been removed. This relaxation process exploits the fact that only a fraction of the physical neighbours of a given disc are in contact with it. Stability is achieved by successively removing contacts with some neighbours and adding them to others.

In a pack of discs such contact re-arrangements require motions of the discs. To avoid such motion we make a restrictive geometric *Ansatz*. We suppose that the beads once assembled have been deformed so that all non-contacting neighbours are nearly in contact. Specifically, we add material to each pair of non-contacting neighbours so that the gap between them is infinitesimal. The remaining gap is a) at the centre of the original gap, b) oriented the same as the original gap and c) proportional to the width of the original gap. Under this *Ansatz* contact rearrangements can occur with arbitrarily little motion. Thus the positions of the beads and the contact angles can be taken as fixed during the relaxation process. The *Ansatz* thus simplifies the relaxation behaviour greatly. It also abstracts the essential process of contact rearrangement from the inessential process of bead motion.

The adaptive network approach has a number of advantages over traditional simulation methods. It operates directly in the limit of infinitely rigid beads, and also in the isostatic limit [12]. That is, the number of contacts is

just sufficient to determine the positions of the beads and the magnitudes of the contact forces. In two dimensions an isostatic pack has on average 4 contacts per bead. A further advantage of using this method is that the linear response regime can be probed directly, a feature that will be exploited in Sec. 4 of the current work. However, the computational resources required do not scale favourably with the number of beads N , with the memory needed varying as $O(N^2)$ and the simulation time increasing as $O(N^4)$. Thus its benefits are restricted to somewhat small piles, typically $N \leq 500$ here.

A sample output from our simulations is given in Fig. 1, which shows a highly polydisperse system with $R_{\max} = 3$ that is first stabilised under a vertical load, and then restabilised under a shearing force angled at 20° to the vertical [13]. The positions of the beads is preserved under the change of load; this is the hallmark of the adaptive network algorithm. However, the network of contact forces adjusts to support the new load, and moreover the strongest contacts have a clear tendency to align with the direction of \mathbf{F}^{ext} . No such alignment is apparent for the weaker bonds. The appearance of concentrated chains of force that align in such a way as to support the load has also been observed in experiments and simulations [14,15,16].

Before presenting our quantitative results, we remark that although the contact forces must be non-tensile, they need not be compressive. Highlighted in Fig. 1 are a small number of contacts with *exactly* zero force. It should be recalled that the beads in the bulk are weightless. In a real packing, these zero-force bonds would be replaced by

weak compressive contacts that are proportional to the weight of a single bead. Physically, these beads occupy a position in the force network that is shielded from the applied load by an ‘arch’ above the bead, and thus play no role in the macroscopic propagation of the stress through the system. In the language of [17], they are *spectator* beads. The proportion of such beads is typically small but finite, roughly 2% for a low polydispersity $R_{\max} = 1.1$, increasing to around 5% for $R_{\max} = 3$. There is also a slight increase in their numbers for sheared systems.

3 The null-stress law

As mentioned in the introduction, there has been considerable recent interest in deriving an equation relating the components of the stress tensor for a granular body [1,8,9,10,18,19]. In this section we test a proposed class of equations against our simulations. Similar results have already been published in [11], but only for low polydispersity. Here we extend the analysis to highly polydisperse systems with $R_{\max} = 3$, thus eliminating concerns over the possible effects of crystallinity.

The stress tensor σ_{ij} generally has 3 independent components in two dimensions (the absence of local torque fixes $\sigma_{xy} = \sigma_{yx}$). Since the forces must balance at every point in the system, σ_{ij} obeys the stress continuity equations

$$\partial_i \sigma_{ij} = F_j^{\text{ext}} \quad . \quad (1)$$

This gives two equations in three unknowns, so an extra equation is required for closure. One proposal for this ‘missing’ equation, called the ‘oriented stress linearity’ model [1] or ‘null stress’ law [10], is that there exists a linear relationship between the σ_{ij} ,

$$\frac{\sigma_{xx}}{\sigma_{yy}} = \eta + \mu \frac{\sigma_{xy}}{\sigma_{yy}} . \quad (2)$$

The coefficients η and μ depend on the construction history of the pile, so μ will vanish if the construction respects left-right symmetry, for example.

To test the proposed equation (2), we plot in Fig. 2 the components of σ_{ij} for systems under differing degrees of shear. Here the σ_{ij} have been averaged over the bulk of the system. This is a valid procedure because, with our geometry and boundary conditions, the σ_{ij} are constant everywhere except the narrow surface layer. It is immediately apparent from the data that $\sigma_{xy}/\sigma_{yy} = F_x^{\text{ext}}/F_y^{\text{ext}}$ to very good precision. This is a trivial result that is easily derived from (1), and can be regarded as a consistency check for our simulations.

More revealing is the data for normal components of the stress, which approximately obey $\sigma_{xx} = \sigma_{yy}$ for un-sheared or slightly sheared systems. This suggests that $\mu = 0$, confirming that our construction procedure preserves left–right symmetry. The linear relationship between σ_{xx} and σ_{yy} breaks down under higher angles of the applied load, indicating that the shear has changed the structure of the system in such a way that μ is no longer zero, and left-right symmetry is violated. (Note that the response within a system that has been stabilised under a

large angle load is still linear, as indeed it must always be for any packing constructed by the adaptive network algorithm). Equation (2) may hold even for large angle shears if μ is some function of the ratio $F_y^{\text{ext}}/F_x^{\text{ext}}$, but our data is too noisy to suggest a meaningful fit.

Additionally, the finding that $\eta \approx 1$ is in agreement with earlier work on weakly polydisperse systems [11]. This suggests that the ‘speed of light’ for stress propagation is approximately 1, irrespective of polydispersity. The analysis of the response function presented in the next section also agrees with this observation. We postpone further discussion of this point until Sec. 5.

4 Response function

The previous section considered only the coarse-grained components of σ_{ij} averaged over the whole bulk of the packing. To gain further insight into the nature of the stress propagation, we now turn to consider the response of the system to an infinitesimal force \mathbf{F}_γ applied to a single bead γ .

The prediction of the equation (2) for this problem is already well documented (see *e.g.* [8,10]), but in brief, the substitution of (2) into the stress continuity equations (1) gives

$$\partial_x(\eta\sigma_{yy} + \mu\sigma_{xy}) + \partial_y\sigma_{xy} = F_x^{\text{ext}} , \quad (3)$$

$$\partial_x\sigma_{xy} + \partial_y\sigma_{yy} = F_y^{\text{ext}} . \quad (4)$$

After some straightforward manipulations, these can be rewritten as

$$(\partial_y - c^+ \partial_x)(\partial_y - c^- \partial_x)\sigma_{ij} = 0 \quad , \quad (5)$$

where $c^\pm = \frac{1}{2}(-\mu \pm \sqrt{\mu^2 + 4\eta})$. These equations are hyperbolic, and as such belong to the same class of equations as the wave equation. Thus they predict that the response to the perturbation should propagate downwards only along the two characteristics, or ‘light rays,’ defined by $\Delta y = c^\pm \Delta x$, where $(\Delta x, \Delta y)$ is the relative displacement from the point of the perturbing force.

If this picture is correct, then only those beads α and β with a point of contact that lies near to one of the light rays can have their contact force altered by the application of the perturbation. To test this prediction, we define the response function $\mathbf{G}(\alpha\beta|\gamma)$ by

$$\Delta f_{\alpha\beta} = \mathbf{G}(\alpha\beta|\gamma) \cdot \mathbf{F}_\gamma \quad , \quad (6)$$

where $\Delta f_{\alpha\beta}$ is the change in the magnitude of the contact force between beads α and β due to the perturbing force \mathbf{F}_γ acting on bead γ . Thus $\mathbf{G}(\alpha\beta|\gamma)$ encodes the response to the force \mathbf{F}_γ without requiring the direction of \mathbf{F}_γ to be specified. Note that for our geometry-preserving procedure, only the magnitude of the contact force can be varied, as the angles were fixed during the initial preparation stage.

$\mathbf{G}(\alpha\beta|\gamma)$ is plotted in Fig. 3 for systems of three different polydispersities that have been stabilised under a vertical load. For the lowest polydispersity $R_{\max} = 1.1$ the response is concentrated along rays radiating at $\approx 45^\circ$ angles, suggesting that $c^\pm \approx \pm 1$. This cannot be due to crystallinity, as the contacts in a close packed two-dimensional

packing lie rather at a 30° angle. For higher polydispersities, the light rays become less distinct due to the increased noise, and the magnitude of $\mathbf{G}(\alpha\beta|\gamma)$ decays more rapidly away from bead γ . However, on length scales of ~ 5 beads diameters or more it is still possible to discern maxima in $\mathbf{G}(\alpha\beta|\gamma)$ along the same 45° lines as before.

To make these observations more quantitative, we plot in Fig. 4 the magnitude of the response $|\mathbf{G}(\Delta x, \Delta y)|$ at different depths Δy below the perturbation. It is evident that the peak response lies near to the lines $\Delta y = \pm \Delta x$, again confirming that $c^\pm \approx \pm 1$. Furthermore, the amplitude of the peaks decays like $(\Delta y)^{-1/2}$, which presumably arises from the diffusive spreading-out of $|\mathbf{G}(\Delta x, \Delta y)|$ with increasing depth [20]. Diffusive spreading should also mean that the width of the peaks increases like $(\Delta y)^{1/2}$, but our data is too noisy to test this claim at present.

It is interesting to compare our results to the recent model of Bouchaud *et al.* which allows the force to propagate along straight rays until they are scattered by a random distribution of defects [21]. These authors found that disorder causes a crossover from a two-peak response function on short length scales to a single-peak, ‘pseudo-elastic’ behaviour on longer scales. By contrast, we have found no evidence of any crossover, and the two-peak form of $|\mathbf{G}(\Delta x, \Delta y)|$ persists to the longest length scales we have been able to simulate. It is not clear if this discrepancy has anything to do with the differing underlying assumptions between the two models, or if we are simply unable to generate sufficiently large systems to observe the crossover.

The response function for systems that have been stabilised under a shearing load are given in Figs. 5 and 6. It is readily apparent that applying the shear does not alter the orientation of the light cone, *i.e.* the characteristics have the same gradients $c^\pm \approx \pm 1$ as in the unsheared system. However, the magnitude of the response becomes stronger along the ray that extends in the same direction as the shear, and weaker along the opposite-pointing ray, as required by (6). With increased polydispersity, there is a greater degree of noise and the weaker ray is eventually lost in the background, as seen in *e.g.* Fig. 5c.

5 Discussion

The central finding of this paper has been the repeated observation of a ‘speed of light’ $c = 1$ for the characteristics along which the stress propagates. This was first inferred from the form of the ‘constitutive equation’ described in Sec. 3, which for unsheared or mildly sheared systems were consistent with $\sigma_{xx} = \eta\sigma_{yy}$ with $\eta = c^2 \approx 1$. Confirmation came from the response functions in Sec. 4, which were concentrated within a ‘light cone’ with a central axis running parallel to gravity. The gradient of the surfaces of this cone were again $c^\pm \approx \pm 1$. In other words, the two characteristics of the hyperbolic equation for stress are nearly orthogonal. Our earlier study [11] indicates that this property survives even when the preparation procedure is not mirror-symmetric. In that case, the null-stress law has the general form $\sigma_{xx} = \eta\sigma_{yy} + \mu\sigma_{xy}$, with the value of η still consistent with 1. As seen from (5), if $\eta = 1$ then the characteristics obey $c^+c^- = -1$ for all μ , *i.e.* they are

orthogonal, just as in the fixed principle axes theorem [9]. The fact that the orthogonality of the characteristics appears to be so robust, demands an explanation.

Equality between the normal stresses $\sigma_{xx} = \sigma_{yy}$ is also found in liquids, where it reflects the isotropic nature of the medium. However, this interpretation cannot be applied to our model, since the construction history and boundary conditions give rise to a system that is anything but isotropic. The anisotropy is most explicit in the response functions plotted in *e.g.* Fig. 3, which clearly show that the orientation of the light cone is fixed with respect to gravity, irrespective of the direction of the perturbing force \mathbf{F}_γ or the degree to which the system is being sheared. Clearly we must look elsewhere for an explanation.

In the absence of a more compelling reason why $c = 1$, we tentatively propose the following explanation. Firstly, observe that the relation $\sigma_{xx} = \sigma_{yy}$ means that the volume of the system is conserved under small perturbations. To see this, consider a system that is contained within a rectangular box of width X and height Y . Let us suppose that, under the action of an external force f_x applied to one of the side walls, the width of the system changes to $X + \delta X$. Similarly, a force f_y is applied to the top of the box, and the height changes to $Y + \delta Y$. If both δX and δY are sufficiently small, the topology of the contact network is not altered during this motion and the perturbation is a ‘soft mode’ [10], meaning that it does not change the total energy of the system and hence has no restoring force. This follows from the isostatic nature of the network; see [10]

for details. To avoid runaway motion, the total work done on the system must vanish, *i.e.* $f_x \delta X + f_y \delta Y = 0$. But the relation $\sigma_{xx} = \sigma_{yy}$ can be rewritten as $f_x/Y = f_y/X$, giving $Y\delta X + X\delta Y = 0$. The left hand side of this equation is just the change in volume of the system, which therefore remains fixed, as claimed.

It is plausible to suppose that our observation of $c = 1$ arises from a state of minimal volume or maximal compaction, as suggested above. This suggests that c may be unity in a broader class of physical systems. Still, we have not demonstrated the necessary conditions for a minimal-volume packing. It may require a random close-packed initial state. It also may require frictionless contacts or regular bead shapes. Further, we have not demonstrated that our simulated bead pack has minimal volume in the requisite sense. Nor have we shown that it would continue to have $c = 1$ if we allowed the beads to move during relaxation. Thus the class of systems with $c = 1$ beyond that presented here cannot be fully characterised at this time.

6 Summary

In summary, we have investigated the propagation of stress through a body of frictionless rigid discs using the adaptive network algorithm. This algorithm first generates a two-dimensional packing via a sequential deposition procedure, and then calculates the contact forces in response to a load applied to the free surface. Tensile bonds are removed by altering the topology of the contact network, in a manner that preserves the mean coordination num-

ber; the packing is always isostatic. This is performed in the linear regime in which bead deformation and motion is neglected, so that although the topology of the network can evolve, the geometry is preserved.

The linear response to a force applied to a single bead was calculated, and was found to propagate in two downward-pointing ‘rays.’ Our central result is that the ‘speed of light’ c of these rays is approximately 1, irrespective of the polydispersity of the bead size distribution, or the degree to which the system is being sheared. We have also argued that $c = 1$ may be understandable if the system naturally adopts a local minimum of volume. Furthermore, we have shown that the magnitude of the response function decays in a way that suggests a diffusive spreading-out with the vertical distance from the source of the perturbation. It would be interesting to see if other microscopic models also scale in a similar manner.

There are many possible directions in which the results presented in this paper can be extended. In particular, we feel that there would be considerable advantages to devising a modified adaptive network algorithm that scales more favourably with system size, whilst still directly probing the linear response regime. This would help to reduce the significant error bars found in some of our data. One way to achieve this might be to change the rule that updates the system when a single bond is changed, which is currently global and requires $O(N^2)$ calculations. Replacing this with a local rule should significantly improve the simulation times and hence the statistics, al-

though it is not clear what approximations such an optimisation would entail.

The current work has focused purely on the problem of stress propagation through granular materials. However, granular media make up only a small subclass of systems that can be described as ‘jammed,’ a class that also includes glasses and foams [22], for example. It has recently been demonstrated that the distribution of inter-bead forces in these systems exhibits a kind of universality when in their jammed state [22]. Clearly the adaptive network algorithm could be a useful probe of the extent and limits of any such universality. Since this is a separate question to that considered in this paper, we will present our results on this issue elsewhere [23].

Acknowledgements

The authors would like to thank Mike Cates and Joachim Wittmer for informative discussions regarding the work presented in this paper. DAH was funded by EPSRC (UK) grant no. GR/M09674. This research was supported in part by the US National Science Foundation through its MRSEC program under award DMR-980859.

References

1. M. E. Cates, J. P. Wittmer, J.-P. Bouchaud and P. Claudin, *Philos. Trans. Roy. Soc. A* **356**, 2535 (1998); also *cond-mat/9803266*.
2. G. Combe and J.-N. Roux, *Phys. Rev. Lett.* **85**, 3628 (2000).
3. L. Vanel, D. Howell, D. Clark, R. P. Behringer and E. Clément, *Phys. Rev. E* **60**, R5040 (1999).
4. R. Brockbank, J. M. Huntley and R. C. Ball, *J. Phys. II* **7**, 1521 (1997).
5. L. Vanel, P. Claudin, J.-P. Bouchaud, M. E. Cates, E. Clément and J. P. Wittmer, *Phys. Rev. Lett.* **84**, 1439 (2000).
6. J. Geng, D. Howell, E. Longhi, R. P. Behringer, G. Reydellet, L. Vanel, E. Clément and S. Luding, preprint *cond-mat/0012127*.
7. G. Reydellet and E. Clément, *Phys. Rev. Lett.* **86**, 3308 (2001).
8. J. P. Wittmer, M. E. Cates and P. Claudin, *J. Phys. I* **7**, 39 (1997).
9. J. P. Wittmer, P. Claudin, M. E. Cates and J.-P. Bouchaud, *Nature* **382**, 336 (1996).
10. A. V. Tkachenko and T. A. Witten, *Phys. Rev. E* **60**, 687 (1999).
11. A. V. Tkachenko and T. A. Witten, *Phys. Rev. E* **62**, 2510 (2000).
12. C. F. Moukarzel, *Phys. Rev. Lett.* **81**, 1634 (1998).
13. Examples of larger systems can be found at <http://www.ph.ed.ac.uk/cmatter/cgi-bin/archive/show.cgi?db=publications&id=73>
14. F. Radjai, D. E. Wolf, M. Jean and J.-J. Moreau, *Phys. Rev. Lett.* **80**, 61 (1998).
15. C.-h. Liu, S. R. Nagel, D. A. Shecter, S. N. Coppersmith, S. Majumdar, O. Narayan and T. A. Witten, *Science* **269**, 513 (1995).
16. D. Howell, R. P. Behringer and C. Veje, *Phys. Rev. Lett.* **82**, 5241 (1999).
17. M.E. Cates, J. Wittmer, J.P. Bouchaud and P. Claudin, *Phys. Rev. Lett.* **81**, 1841 (1999).
18. O. Narayan, *Phys. Rev. E* **63**, 010301 (2001).
19. O. Narayan and S. R. Nagel, *Physica A* **264**, 75 (1999).

20. P. Claudin, J.-P. Bouchaud, M. E. Cates and J. P. Wittmer, Phys. Rev. E **57**, 4441 (1998).
21. J.-P. Bouchaud, P. Claudin, D. Levine and M. Otto, Euro. Phys. J. E **4**, 451 (2001).
22. C. S. O’Hern, S. A. Langer, A. J. Liu and S. R. Nagel, Phys. Rev. Lett. **86**, 111 (2001).
23. D. A. Head, A. K. Tkachenko and T. A. Witten, in preparation.

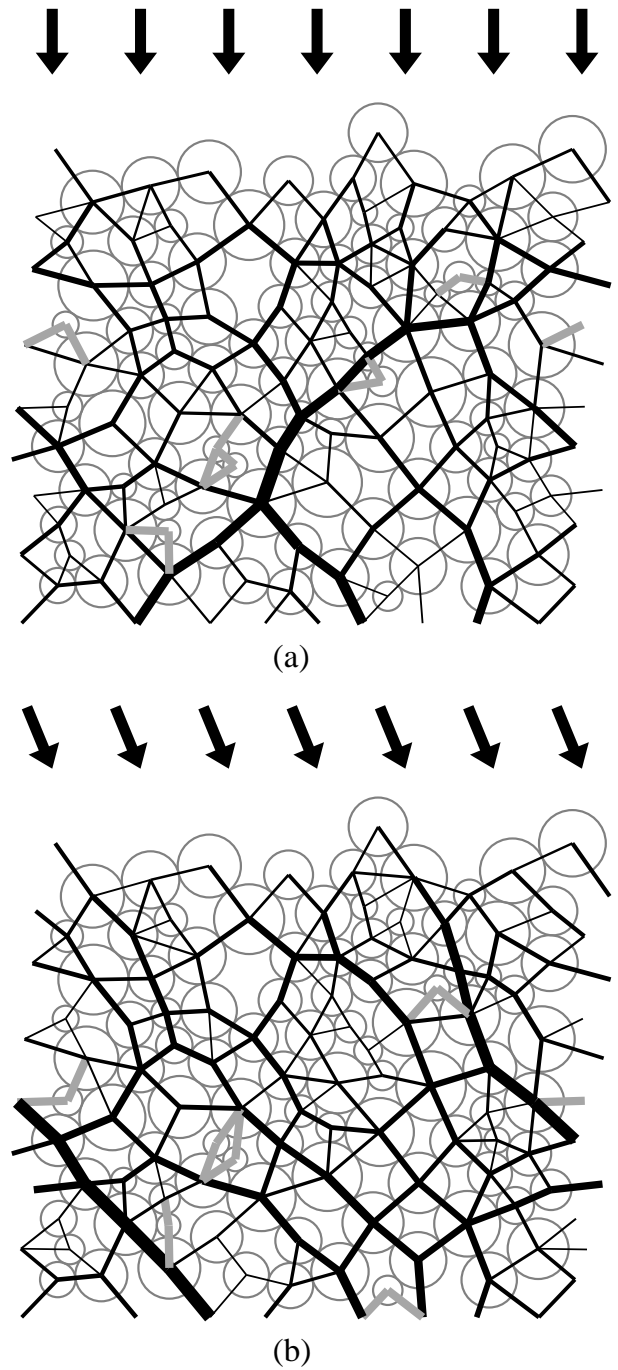


Fig. 1. Sample output of the adaptive network algorithm for a system subjected to (a) a vertical load, and (b) for the same packing under a shear of approximately 20° . The arrows point in the direction of the loading force \mathbf{F}^{ext} . The black lines between beads denote compressive contacts, with a force whose magnitude is proportional to the thickness of the line. The thick gray lines represent tenuous contacts of exactly zero force. Note that contacts between slightly separated beads are al-

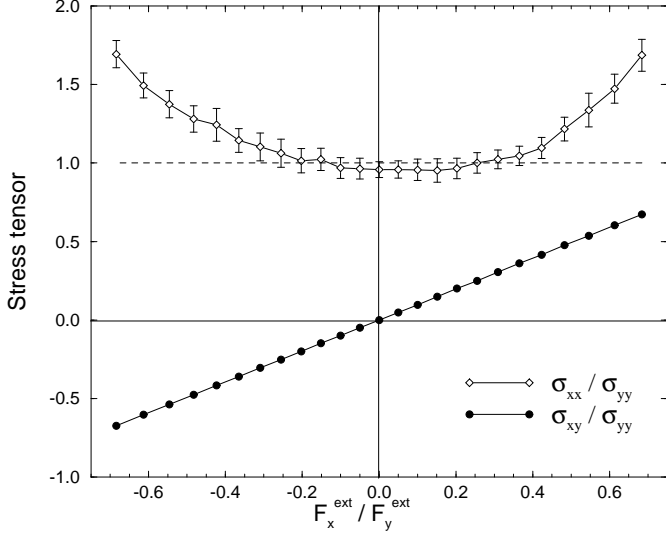


Fig. 2. The components of the stress tensor σ_{ij} as a function of the applied shear for an $N = 400$ bead system of polydispersity $R_{\max} = 3$. The error bars for the σ_{xx}/σ_{yy} points are the standard deviation over 25 different packings. For comparison, the dashed line represents $\sigma_{xx} = \sigma_{yy}$. The σ_{xy}/σ_{yy} data lie on a line of slope 1 and the errors are smaller than the symbols.

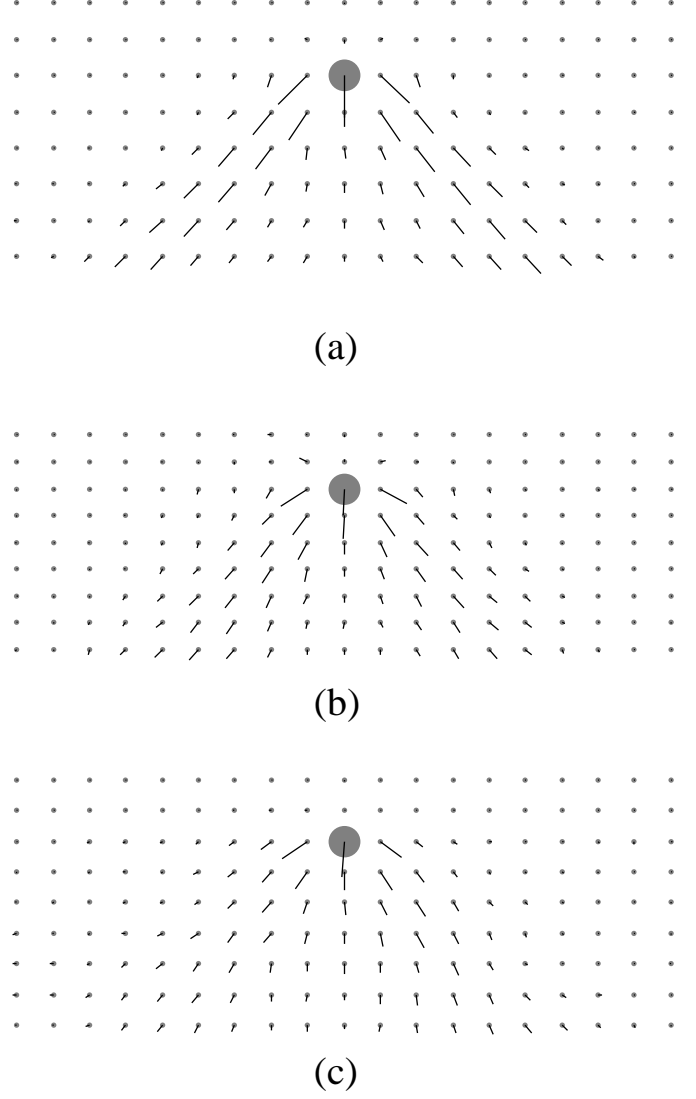
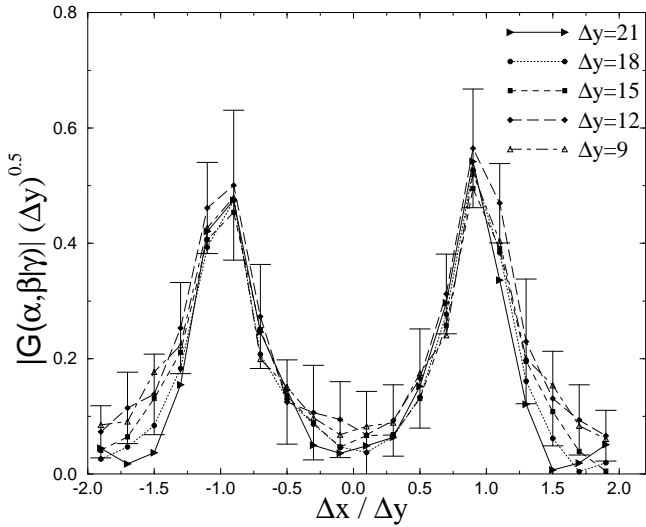
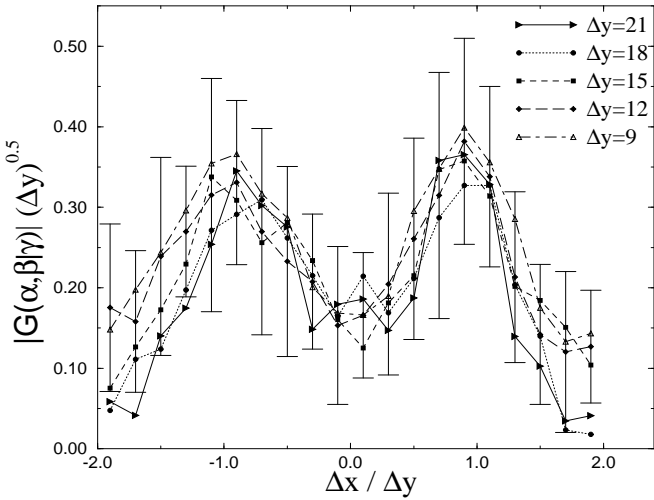


Fig. 3. The coarse-grained response function $\mathbf{G}(\alpha|\gamma)$ for packings under a vertical load and with polydispersity (a) $R_{\max} = 1.1$, (b) $R_{\max} = 1.5$ and (c) $R_{\max} = 3$. Here, $\mathbf{G}(\alpha|\gamma)$ has been averaged over all those beads γ whose centres lie in a narrow horizontal strip approximately two thirds of the way up the pile. This central bead is represented by the large grey filled circle. The vectors shown represent $\mathbf{G}(\alpha|\gamma)$ as a function of the relative displacement $(\Delta x, \Delta y)$ from the centre of bead γ to the point of contact between beads $\alpha \leftrightarrow \beta$. Each vector points away from the small grey circle. The data was averaged over 100 runs of $N = 500$ beads. Each mesh point is separated by 1.5 bead diameters.

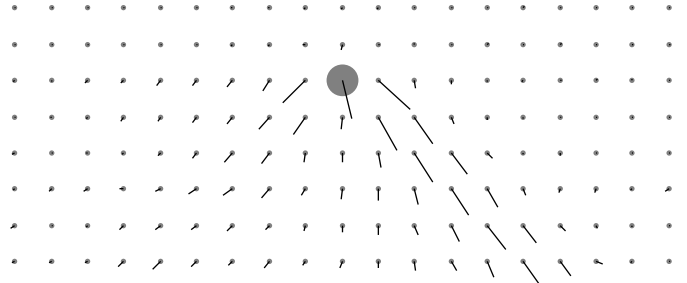


(a)

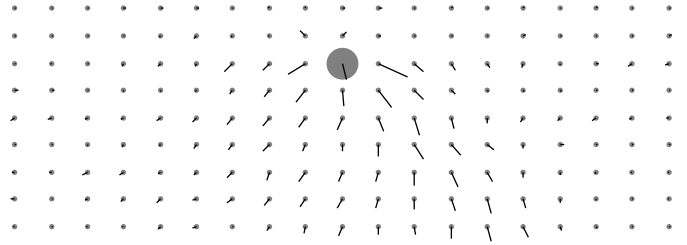


(b)

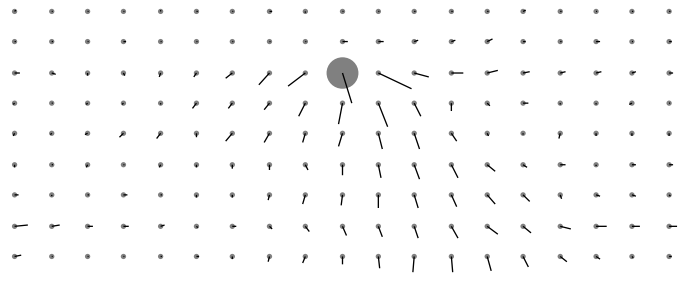
Fig. 4. The magnitude of the response function $|G(\alpha, \beta|\gamma)|$ scaled up by a factor $(\Delta y)^{1/2}$, plotted against $\Delta x/\Delta y$, where $(\Delta x, \Delta y)$ is the relative displacement from the source of the perturbation measured in units of the mean bead radius. Positive Δy correspond to points *below* the source. Each line represents the average over a horizontal strip of width 3, with a mean Δy as indicated in the legend. The polydispersity was (a) $R_{\max} = 1.1$ and (b) $R_{\max} = 1.5$, and $N = 500$ in both



(a)



(b)



(c)

Fig. 5. The response function $G(\alpha|\beta|\gamma)$ when the applied load is angled at 20° to the right of the vertical, for polydispersities (a) $R_{\max} = 1.1$, (b) $R_{\max} = 1.5$ and (c) $R_{\max} = 3$.

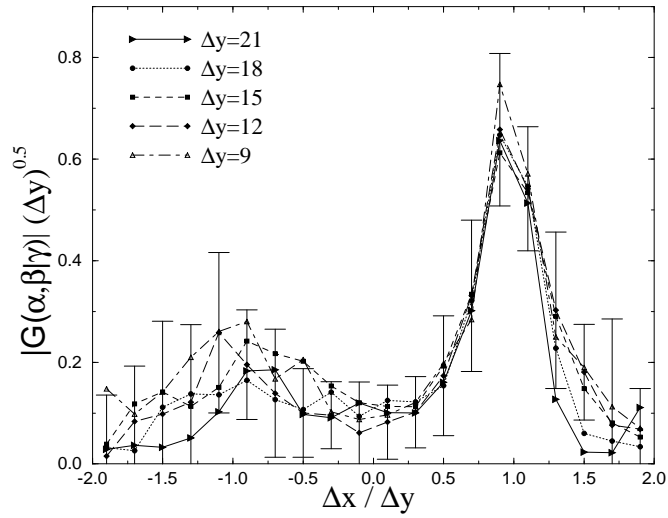


Fig. 6. The same as Fig. 4 for a system under a shearing load, angled at 20° to the vertical. Only the results for weakly polydisperse system $R_{\max} = 1.1$ is given, as the error bars were much larger than the data points for higher polydispersities.

